http://www.jstage.jst.go.jp/browse/biophysics

BIOPHYSICS

Vol. 11, pp. 47–53 (2015)
doi: 10.2142/biophysics.11.47

Lever arm extension of myosin VI is unnecessary for the adjacent binding state

Keigo Ikezaki[1,2], Tomotaka Komori[1], Yoshiyuki Arai[3] and Toshio Yanagida[1,2,4,5]

[1]*Graduate School of Frontier Biosciences, Osaka University, Yamadaoka, Suita, Osaka 565-0871, Japan*
[2]*Quantitative Biology Center (QBiC), RIKEN, Furuedai, Suita, Osaka 565-0874, Japan*
[3]*Institute of Scientific and Industrial Research, Osaka University, 8-1 Mihogaoka, Ibaraki, Osaka 567-0047, Japan*
[4]*Center for Information and Neural Networks (CiNet), Yamadaoka, Suita, Osaka 565-0871, Japan*
[5]*WPI, Immunology Frontier Research Center, Osaka University, Yamadaoka, Suita, Osaka 565-0871, Japan*

Received August 19, 2014; accepted December 21, 2014

Myosin VI is a processive myosin that has a unique stepping motion, which includes three kinds of steps: a large forward step, a small forward step and a backward step. Recently, we proposed the parallel lever arms model to explain the adjacent binding state, which is necessary for the unique motion. In this model, both lever arms are directed the same direction. However, experimental evidence has not refuted the possibility that the adjacent binding state emerges from myosin VI folding its lever arm extension (LAE). To clarify this issue, we constructed a myosin VI/V chimera that replaces the myosin VI LAE with the IQ3-6 domains of the myosin V lever arm, which cannot fold, and performed single molecule imaging. Our chimera showed the same stepping patterns as myosin VI, indicating the LAE is not responsible for the adjacent binding state.

Key words: molecular motors, single molecule imaging, molecular structures, molecular functions, genetic engineering

Myosin VI is an ATP hydrolysis coupled motor protein involved in many cellular functions including endocytosis, protein secretion and the maintenance of both the Golgi morphology and stereocilia [1]. It is a unique myosin in that it moves to the minus end of an actin filament [2], while all other myosins move to the plus end [3]. Recently, we proposed that myosin VI moves using three types of steps: large and small forward steps (minus end directed), and backward steps (plus end directed) [4–6]. We introduced the adjacent binding state to explain how myosin VI generates the small steps and backward steps. In this state, both lever arms point the same direction to achieve an inter-head distance of less than 10 nm (parallel lever arms model; Fig. 1A) [4,5]. However, an alternative explanation of the adjacent binding state has the lever arm fold by the Lever Arm Extension (LAE) [7,8], which is unique to myosin VI (LAE folding model; Fig. 1B).

To clarify which model is correct, we constructed a myosin VI/V chimera in which the LAE was substituted for the IQ3-6 domains of the myosin V lever arm. This chimera should be able to generate small steps or backward steps by taking the adjacent binding state only according to the parallel lever arms model. We therefore measured chimera steps at the single molecule level by single molecule fluorescence imaging using total internal reflection fluorescence microscopy and found that the mutant generated small and backward steps like those of myosin VI. This result demonstrates folding of the LAE is not necessary and suggests the adjacent binding state occurs by directing both lever arms the same direction.

Corresponding authors: Tomotaka Komori, Graduate School of Frontier Biosciences, Osaka University, 1-4 Yamadaoka, Suita, Osaka 565-0871, Japan. e-mail: komotomo@gmail.com; Toshio Yanagida, Graduate School of Frontier Biosciences, Osaka University, 1-4 Yamadaoka, Suita, Osaka 565-0871, Japan. e-mail: yanagida@fbs.osaka-u.ac.jp

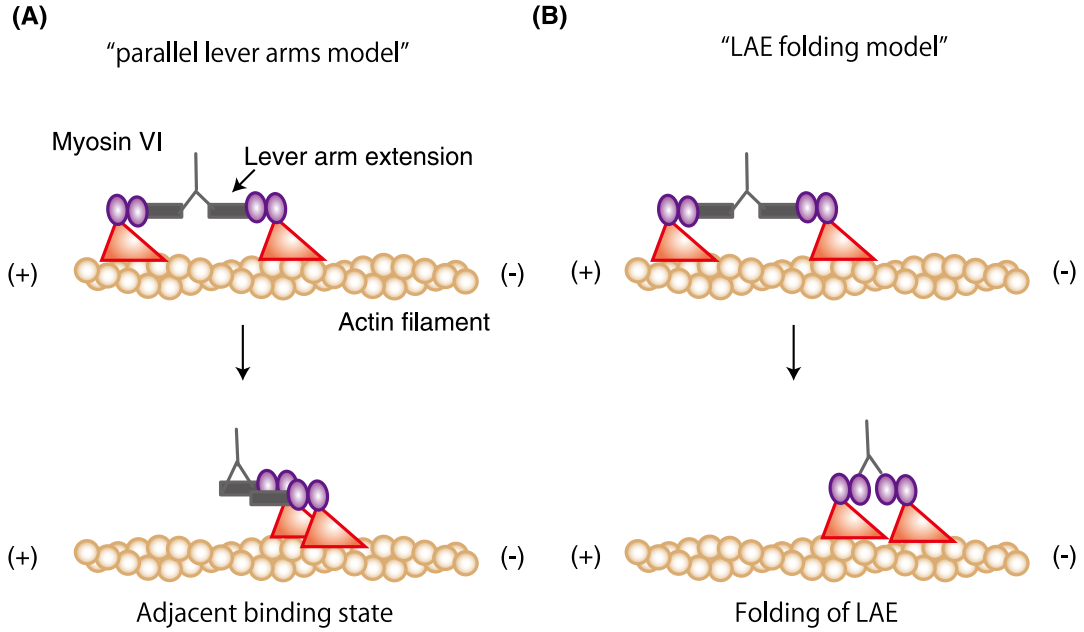

Figure 1 Two models for the adjacent binding state. (A) In the parallel lever arms model, myosin VI takes the adjacent binding state by directing both lever arms the same direction. (B) In the lever arms folding model, myosin VI takes the adjacent binding state by folding the lever arm extension (LAE).

Materials and Methods

Preparation of protein samples

Human myosin Va cDNA (product ID: ORK07567), human myosin VI cDNA (product ID: ORK01080) and human calmodulin cDNA (product ID: ORK01403) were purchased from Kazusa DNA, Japan. To create myosin VI/V chimera constructs, myosin VI cDNA (1 to 830 amino acids) was introduced into pFastBac (Life Technologies) to make a baculovirus. This myosin VI fragment included the motor domain, the unique myosin VI insertion and the core of the IQ domain (see Results for definition). For biotin labeling, a HaloTag (Promega) fragment was attached at the N-terminal of myosin VI via the linker. To construct the myosin VI/V chimera, myosin V cDNA (807 to 1099 amino acids) was inserted after the above myosin VI sequence using the In-Fusion HD cloning kit (Clontech). This myosin V fragment included the lever arm domain just after the IQ2 motif and coiled-coil domain (Fig. 2A, B). Furthermore, a GCN4 sequence, which ensures dimerization, and His6-tag, which enables affinity protein purification, were also inserted at the C-terminus (Fig. 2A). Calmodulin was introduced into another pFastBac plasmid, and myosin VI/V chimeras were expressed using sf9 cells and two kinds of baculoviruses from the above pFastBac plasmids. For myosin VI expression and purification, myosin VI cDNA (1-1021) and calmodulin were introduced into a single pFastBac Dual plasmid (Life Technologies). A HaloTag was attached at the N-terminal of myosin VI, while GCN4, SNAP-Tag and His6-tag were attached at the C-terminal.

Protein purification was performed as previously described [4,5]. During the purification, myosin VI/V chimeras or myosin VI were biotinylated at the HaloTag using a biotin-halo-ligand. Qdot585 streptavidin conjugates and biotinylated myosin VI/V chimeras or myosin VI were incubated as previously described [6] for single molecule fluorescence imaging.

Microscopy observation and analysis

All experiments were performed according to previously reported methods [6]. Briefly, a 10 µl volume microchamber was made by placing a small coverslip (18×18 mm, No. 1 Thickness, Matsunami, Japan) over a larger one (22×32 mm, No. 1 thickness, Matsunami) using double-sided adhesive tape (50 µm thickness). Next, 1.5 mg/ml actinin (Sigma-Aldrich) in assay buffer (AB: 20 mM HEPES-KOH pH 7.8, 25 mM KCl, 5 mM $MgCl_2$ and 1 mM EGTA) was adsorbed onto the glass surface, followed by a 3 min incubation, a 20 µl AB wash, and finally an injection of 2 µg/ml non-fluorescent phalloidin labeled actin filament solution in AB into the chamber. After another 3 min incubation and 20 µl AB wash, 5 mg/ml α-casein in AB was injected into the chamber. After a 3 min incubation and 20 µl AB wash, motility buffer (MB: AB plus an oxygen scavenger system, ATP regeneration system, 20 µg/ml calmodulin and 100 µM ATP) mixed with Qdot585-labeled myosin VI/V chimeras was flowed into the chamber, and the chamber was sealed with nail polish. Qdot585-conjugated myosin VI/V chimeras were imaged using total internal reflection fluorescence microscopy (TIRFM), and the corresponding fluorescent images were captured with an EMCCD camera (Andor iXon).

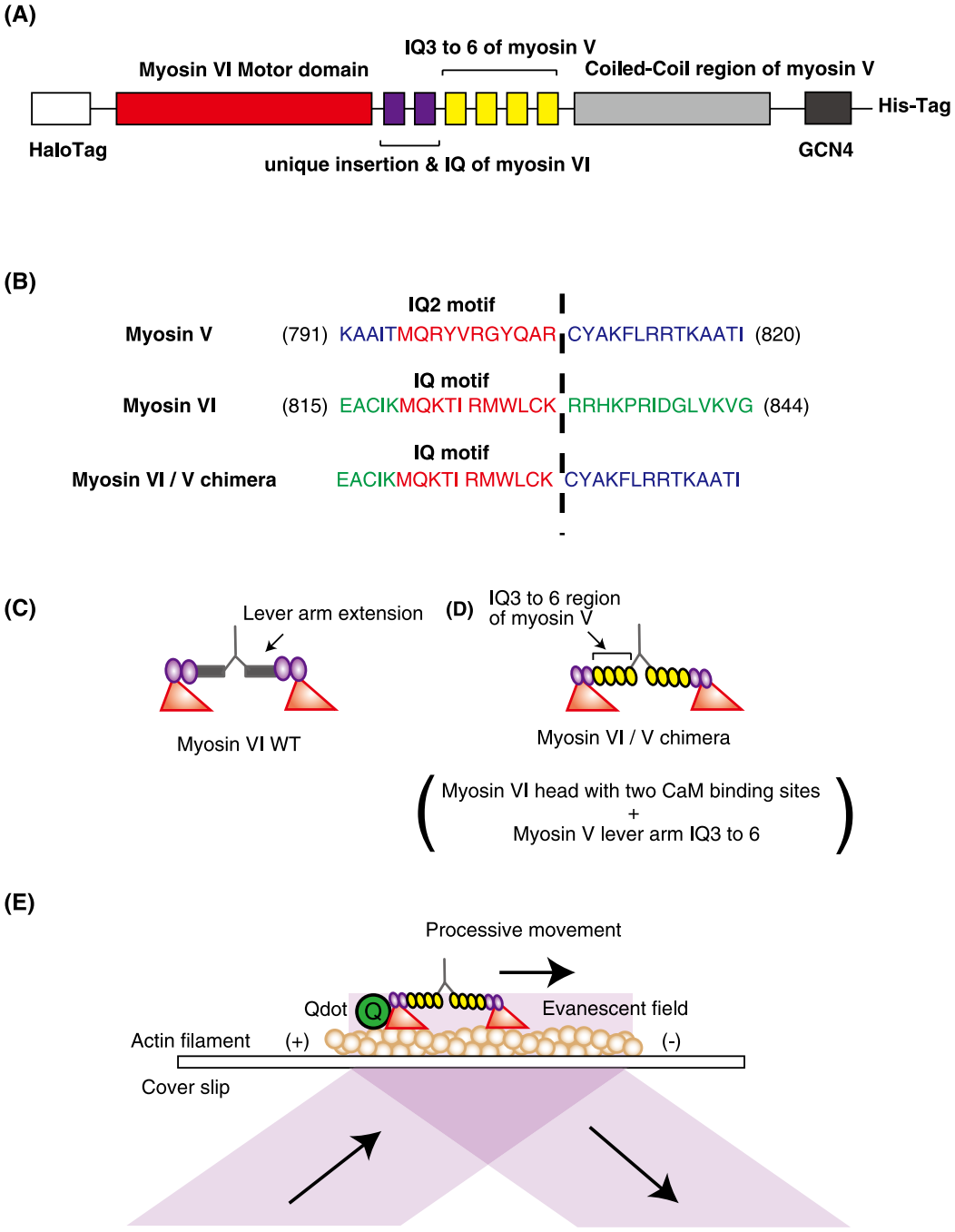

Figure 2 The myosin VI/V chimera construct and experimental setup for observing chimera steps. (A) Schematic drawing of each domain in the myosin VI/V chimera. (B) The amino acid sequence around the junction between myosin VI and V in the chimera. The myosin V sequence (CYAKF….) immediately after its IQ2 motif (MQRYVRGYQAR) was inserted just after the myosin VI IQ motif (MQKTIRMWLCK). (C, D) Schematic drawings of myosin VI (C) and the chimera (D). The motor domain, calmodulin binding to the myosin VI sequence, calmodulin binding to the myosin V sequence and LAEs are described in red, purple, yellow and grey, respectively. (E) Cartoon of Qdot 585-labeled chimeras moving along an actin filament based on total internal reflection microscopy (TIRFM) observations. Images not to scale.

Data analysis

The center of a fluorescent spot in each frame was determined using a two-dimensional Gaussian fit according to a published method [9] using the custom written ImageJ plugin "PTA" (https://github.com/arayoshipta/projectPTAj). Steps were detected using a MATLAB program for Kerssemaker's chi-square based algorithm [10]. Distributions of steps were fitted to Gaussian functions using OriginLab, while dwell times and run lengths distributions were fitted to exponential decay functions.

Results

Experimental setup

To clarify whether the folding of the myosin VI LAE is responsible for the adjacent binding state, we constructed myosin VI/V chimeras where amino acids 1–830 of myosin VI were followed by amino acids 807–1099 of myosin V (Fig. 2A–D). Calmodulins bind to a myosin lever arm by mainly recognizing the IQ-motif of the consensus sequence of I(L/M)Q xxx RG(M) xxxR(K) amino acids with X being any amino acids sequence as reviewed [11,12]. In myosin VI, the core amino acids sequence of the IQ motif (MQKTIRMWLCK) ends at 830 a.a., while the core amino acids sequence of the IQ2 motif (MQRYVRGYQAR) in myosin V ends at 806 a.a. Since in this study we used chimeras, the amino acids sequence between the IQ motif of myosin VI and the IQ3 motif of myosin V is the same as that between the IQ2 and IQ3 motif in myosin V, meaning that there exists no excessive or shortage of amino acids, which might otherwise compromise calmodulin binding capacity or rigidity of the lever arms. We evaluated the amount of bound calmodulin using SYPRO Red Protein Gel Stain and 4–15% acrylamide SDS-PAGE gels (Supplementary Fig. S1). The ratio of calmodulin on myosin V to myosin VI/V chimera was 1:1.3, indicating that myosin VI/V chimera retain their binding capacity to calmodulin and have rigid lever arms like that of myosin V.

To visualize the stepping motion of the chimeras at the single molecular level, the N-terminus was labeled with Qdot585 using HaloTag, biotin-Halo ligand and streptavidin-coated Qdot585 (Fig. 2E). Here, one of the two motor domains of myosin VI/V chimera was labeled with a Qdot585. Since the Qdot labeling of both myosin motor domains was a rare event [5], we could observe movement with single molecule resolution using TIRFM (Fig.3B).

Motile properties of myosin VI /V chimeras

Myosin VI/V chimeras generated processive steps that included three step types: large steps of 68 nm, small steps of 32 nm and backward steps of –34 nm (Fig. 3B and 4; Supplementary Movie S2). These steps were very similar to those previously reported for myosin VI: 76 nm, 41 nm and –40 nm (Fig. 3A; Supplementary Movie S1) [4]. Furthermore, since a single trace of myosin VI or myosin V/VI chimera contains all three step types, we could confirm that one of the two motor domains of the myosin VI/V chimera was labeled with a single Qdot and that the small and backward steps were not caused by Qdot-labeling of both motor domains from the

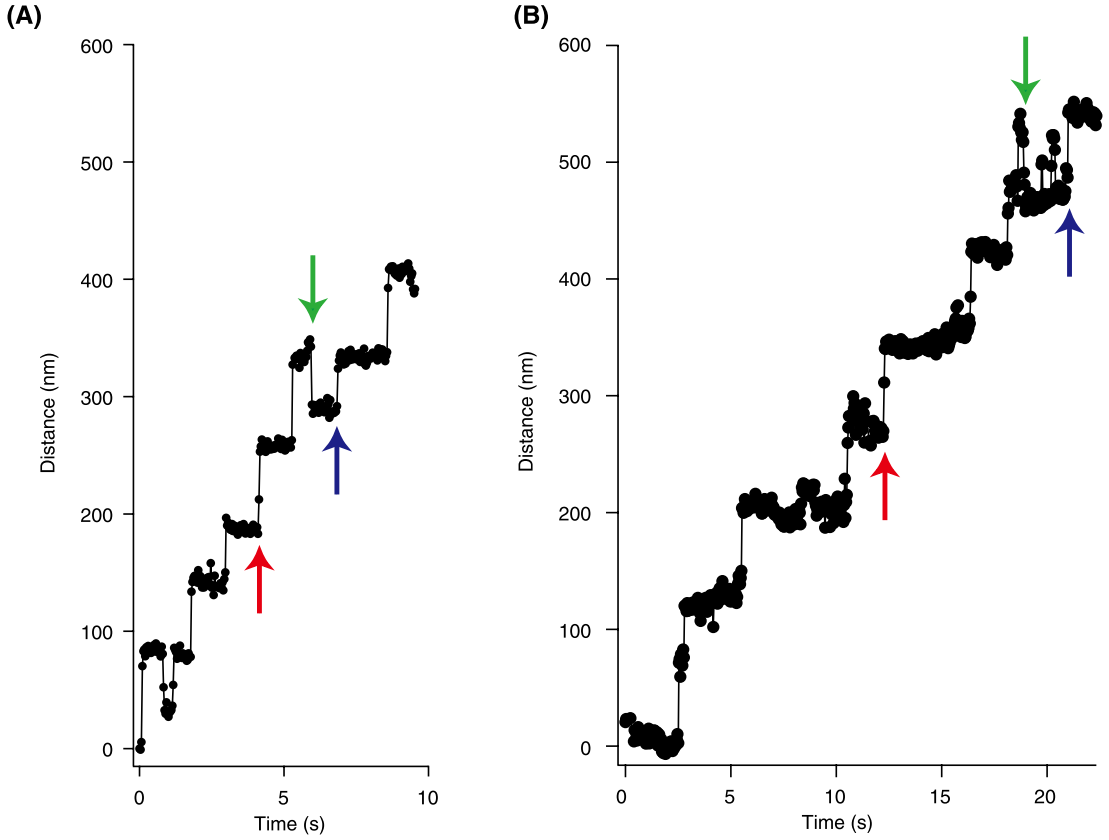

Figure 3 Stepping traces of myosin VI and chimeras. (A) Stepping trace of myosin VI. Examples of large, small and backward steps are indicated by the red, blue and green arrows, respectively. (B) Same as (A) but for the chimera.

same chimera or an aggregation of myosin VI/V chimeras.

The run length of the myosin VI/V chimera (81 nm; Fig. 5A) was less than half the previously reported run length of myosin VI (~200 nm) [4]. Processive movement in myosin is often considered the result of coordinating the ATP-hydrolysis cycle between the two motor domains via intramolecular strain [11]. We concluded that removing the LAE lowered the intramolecular strain and thus the run length too. However, a previous study examining chimera mutants of myosin V that retained the SAH (single alpha helix) domain, which is equivalent to the myosin VI LAE domain, from the dictyostelium myosin MyoM, had lower intramolecular strain because of decreased rigidness in the lever arm region [13]. The lower intramolecular strain seen in our myosin VI/V chimera despite a more rigid lever arm can be explained by the actomyosin geometry [14].

The rate constants of the large, small and backward steps of our chimera were 1.3 s^{-1}, 2.2 s^{-1} and 1.3 s^{-1} at 100 µM ATP, respectively (Fig. 5B–D), while those of myosin VI were about 3 s^{-1} for all step types at 100 µM ATP [6]. The decreased stepping rates for the myosin VI/V chimera might be explained by the reduced intramolecular strain. At 100 µM ATP, the rate limiting process for myosin VI stepping is ATP binding to the rear motor domain [15]. This binding is accelerated by intramolecular strain [16]. Therefore, since the intramolecular strain was decreased in our chimeras, we concluded it caused the ATP-binding rate in myosin VI/V chimera to decrease.

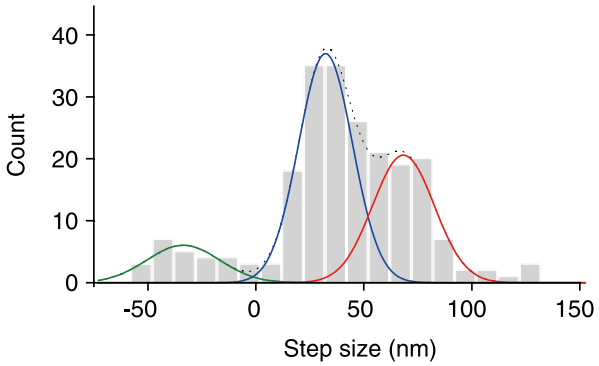

Figure 4 Distribution of chimera steps. The step size distribution of the myosin VI/V chimera at 100 µM ATP was fitted with the convolution of three Gaussian functions (black dashed line) of –34±17 (green solid line), 32±13 (blue solid line) and 68±15 (the red solid line) (mean±standard deviation (nm); n=219).

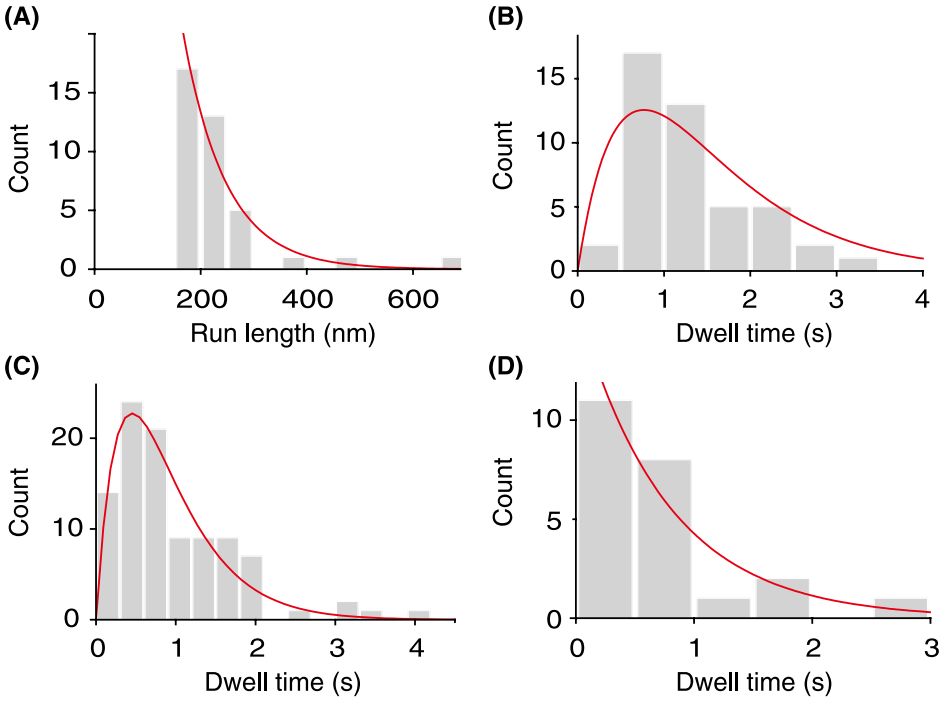

Figure 5 Distribution of dwell times and run lengths of the chimera. (A) The run length distribution of the myosin VI/V chimera at 100 µM ATP over 150 nm was fitted with a single exponential function of mean±standard error (s.e.) = 81±12 nm (n=38). (B–D) The dwell time distributions of the myosin VI/V chimera for large (B) and small steps (C) at 100 µM ATP were fitted with a convolution of two exponentials for successive steps of the same rate constant (Atk^2exp^{-kt}; t = dwell time, k=mean rate constant) of mean rate constants±s.e.=1.3±0.32 s^{-1} (n=45) and 2.2±0.10 s^{-1} (n=99), while that for backward steps (D) was fitted with a single exponential decay function ($A\ exp^{-kt}$; t=dwell time, k = mean rate constant) of mean rate constant±s.e. = 1.3±0.34 s^{-1} (n=23). Since the rate limiting state for myosin VI stepping at 100 µM ATP is the ATP-binding rate, this rate constant is consistent with rate ATP binds to the motor domain of the myosin VI/V chimera.

Discussion

We previously reported that myosin VI can generate three kinds of steps (large, small and backward steps) by taking the adjacent binding state [4,5]. We explained this state using the parallel lever arms model (Fig. 1A). The model is based on measurements of the lever arm length during myosin VI stepping using gold nano particles and dark field imaging of the N-terminus position [4] and the simultaneous tracking of both the C-terminus and N-terminus positions using SHREC [5]. However, the adjacent binding state can also be explained by folding of the LAE (Fig. 1B). We therefore prepared a myosin VI/V chimera mutant that substitutes the LAE with the IQ3-6 domains of myosin V (Fig. 2) and performed single molecule fluorescence imaging, finding that our chimera can generate similar small and backward steps to those of myosin VI (Fig. 3B and Fig. 4). Unlike the LAE, the IQ3-6 is rigid, indicating the adjacent binding state is not the consequence of lever arm folding. Thus, we concluded the parallel lever arms model explains this state (Fig. 3B).

The parallel lever arms model assumes the two lever arms point the same direction, which may help explain why the adjacent binding state is seen in myosin VI [4], but not in myosin V [9]. The lever arms in myosin VI are angled at about 180 degrees from each other [14], while in myosin V it is a much more modest 70 degrees (Supplementary Fig. S2) [17,18]. Because the 180 degree angle is attributed to the unique insertion of myosin VI [17], our chimera, which includes the insertion, should show the same angle. These differences may reflect differences in steric hindrance between the arms, as the adjacent binding state can only occur when the hindrance is low.

In a cell, myosin V, which cannot take the adjacent binding state, has been reported to function as a transporter. On the other hand, myosin VI, which can take the adjacent binding state, has been reported to function as a transporter and as an anchor. Since the adjacent binding state is unique to myosin VI, it may contribute to this second function. Indeed, the adjacent binding state can equally divide the external force onto both its motor domains. Part of the reason for this ability is that the lever arms are parallel in the adjacent binding state, so that both lever arms can take the postpower stroke state [4,5]. It was reported using myosin V that the motor domain in the prepower stroke state spontaneously detaches from actin at a rate of $1\ s^{-1}$ [19] and has weaker actomyosin binding than the postpower stroke state, which suggests the adjacent binding state would be ideal for anchoring function. One might worry that the ATP-binding rate for the postpower stroke state is higher than that for the prepower stroke state under no external load condition. However, an optical trapping study suggested that the ATP-binding rate dramatically slows when an external force is applied to the motor domains [20], meaning that the ATP-binding rate in the adjacent binding state is expected to decrease with external load.

Acknowledgements

K. I. is supported by a research fellowship from JSPS, Japan. We thank the members of QBiC for valuable discussions, R. Kawaguchi for technical help and P. Karagiannis (RIKEN, QBiC) for helpful discussions and comments on the manuscript. This work was supported by a Grant-in-Aid for JSPS Fellows 24-2619 (to K. I.) and a Grant-in-Aid for Young Scientists (B) 25840063 (to T. K.) from MEXT, Japan and RIKEN QBiC, Japan (to T. Y.).

References

[1] Sweeney, H. L. & Houdusse, A. What can myosin VI do in cells? *Curr. Opin. Cell Biol.* **19**, 57–66 (2007).
[2] Wells, A. L., Lin, A. W., Chen, L. Q., Safer, D., Cain, S. M., Hasson, T., Carragher, B. O., Milligan, R. A. & Sweeney, H. L. Myosin VI is an actin-based motor that moves backwards. *Nature* **401**, 505–508 (1999).
[3] Hartman, M. A. & Spudich, J. A. The myosin superfamily at a glance. *J. Cell Sci.* **125**, 1627–1632 (2012).
[4] Nishikawa, S., Arimoto, I., Ikezaki, K., Sugawa, M., Ueno, H., Komori, T., Iwane, A. H. & Yanagida, T. Switch between large hand-over-hand and small inchworm-like steps in myosin VI. *Cell* **142**, 879–888 (2010).
[5] Ikezaki, K., Komori, T., Sugawa, M., Arai, Y., Nishikawa, S., Iwane, A. H. & Yanagida, T. Simultaneous observation of the lever arm and head explains myosin VI dual function. *Small* **8**, 3035–3040 (2012).
[6] Ikezaki, K., Komori, T. & Yanagida, T. Spontaneous detachment of the leading head contributes to myosin VI backward steps. *PLoS ONE* **8**, e58912 (2013).
[7] Spink, B. J., Sivaramakrishnan, S., Lipfert, J., Doniach, S. & Spudich, J. A. Long single alpha-helical tail domains bridge the gap between structure and function of myosin VI. *Nat. Struct. Mol. Biol.* **15**, 591–597 (2008).
[8] Mukherjea, M., Llinas, P., Kim, H., Travaglia, M., Safer, D., Ménétrey, J., Franzini-Armstrong, C., Selvin, P. R., Houdusse, A. & Sweeney, H. L. Myosin VI dimerization triggers an unfolding of a three-helix bundle in order to extend its reach. *Mol. Cell* **35**, 305–315 (2009).
[9] Yildiz, A., Forkey, J. N., McKinney, S. A., Ha, T., Goldman, Y. E. & Selvin, P. R. Myosin V walks hand-over-hand: single fluorophore imaging with 1.5-nm localization. *Science* **300**, 2061–2065 (2003).
[10] Kerssemakers, J. W. J., Munteanu, E. L., Laan, L., Noetzel, T. L., Janson, M. E. & Dogterom, M. Assembly dynamics of microtubules at molecular resolution. *Nature* **442**, 709–712 (2006).
[11] Cheney, R. E. & Mooseker, M. S. Unconventional myosins. *Curr. Opin. Cell Biol.* **4**, 27–35 (1992).
[12] Bähler, M. & Rhoads, A. Calmodulin signaling via the IQ motif. *FEBS Lett.* **513**, 107–113 (2002).
[13] Baboolal, T. G., Sakamoto, T., Forgacs, E., White, H. D., Jackson, S. M., Takagi, Y., Farrow, R. E., Molloy, J. E., Knight, P. J., Sellers, J. R. & Peckham, M. The SAH domain extends the functional length of the myosin lever. *Proc. Natl. Acad. Sci. USA* **106**, 22193–22198 (2009).
[14] Sakamoto, T., Yildez, A., Selvin, P. R. & Sellers, J. R. Step-size is determined by neck length in myosin V. *Biochemistry* **44**, 16203–16210 (2005).
[15] De La Cruz, E. M., Ostap, E. M. & Sweeney, H. L. Kinetic mechanism and regulation of myosin VI. *J. Biol. Chem.* **276**,

32373–32381 (2001).
[16] Pylypenko, O., Song, L., Squires, G., Liu, X., Zong, A. B., Houdusse, A. & Sweeney, H. L. Role of insert-1 of myosin VI in modulating nucleotide affinity. *J. Biol. Chem.* **286**, 11716–11723 (2011).
[17] Ménétrey, J., Llinas, P., Mukherjea, M., Sweeney, H. L. & Houdusse, A. The structural basis for the large powerstroke of myosin VI. *Cell* **131**, 300–308 (2007).
[18] Spudich, J. A. & Sivaramakrishnan, S. Myosin VI: an innovative motor that challenged the swinging lever arm hypothesis. *Nat. Rev. Mol. Cell Biol.* **11**, 128–137 (2010).
[19] Purcell, T. J., Sweeney, H. L. & Spudich, J. A. A force-dependent state controls the coordination of processive myosin V. *Proc. Natl. Acad. Sci. USA* **102**, 13873–13878 (2005).
[20] Chuan, P., Spudich, J. A & Dunn, A. R. Robust mechanosensing and tension generation by myosin VI. *J. Mol. Biol.* **405**, 105–112 (2011).